Table 1. The Changes of the Phosphate Fractions of Blood during Glycolysis *in vitro*

Time (hr.)	Glucose (mgm. per cent)	Inorganic phosphate (mgm. per cent)	Hydrolysable with ease (mgm. per cent)	Hydrolysable with difficulty (mgm. per cent)	Non-hydrolysable (mgm. per cent)	Acid-insoluble (mgm. per cent)
0	119	2·69	5·15	3·44	15·32	10·70
3	78	2·59	5 12	2 85	15·25	10·20
6	31	4·45	3·65	3·35	14 22	10·20
9	20	9·30	3·41	2·61	11·23	9·20
12	16	21·30	0·20	0·97	6·6	9·40
24	12	26·50	0·10	1·13	1·85	9·20

sprayed with Hanes–Isherwood acid molybdate solution[7]. After hydrolysis the chromatograms were treated with a solution of tin chloride[8].

It was found, as observed by Rohdewald and Weber[9], that the acid-soluble phosphorus fraction of human blood contains adenosine triphosphate, fructose-1,6-diphosphate, triosephosphate (mainly 2,3-diphosphoglyceric acid) in addition to inorganic phosphate (Fig. 1). During glycolysis in blood a decrease amounting to total disappearance of adenosine triphosphate, fructose-diphosphate, triosophosphate and a large increase of inorganic phosphate were observed (Table 1, Fig. 1). The inorganic phosphate was released by the progressive hydrolysis of the organic phosphate esters when the blood-glucose concentration fell below 20 mgm. per cent. No significant or substantial changes were found in the acid-insoluble phosphate fraction of blood, which points to the fact that the acid-insoluble organic phosphate compounds probably do not participate directly in the metabolic pathways of phosphorus during glycolysis in blood.

Acknowledgments are made to Messrs. Sigma Chemical Company, St. Louis, for supplying the samples of adenosine triphosphate and adenosine diphosphate. I thank Miss M. Vanščák for technical assistance.

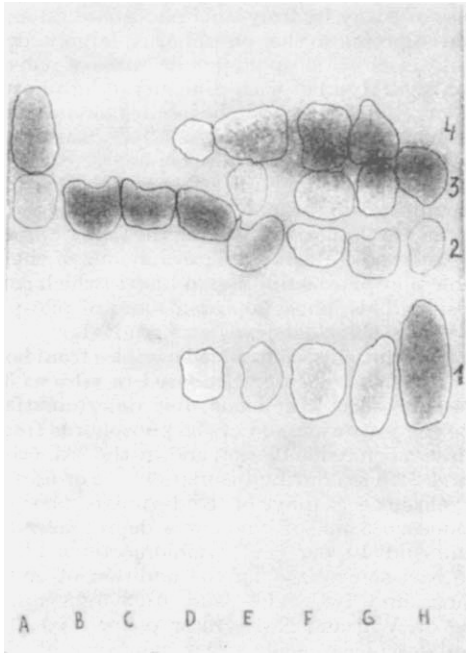

Fig. 1. The paper chromatogram of acid-soluble phosphorus compounds of blood during glycolysis in blood. The spots of known organic phosphate esters (*A*, *H* columns): (1) adenosine triphosphate, (2) inorganic phosphate, (3) fructose-1,6-diphosphate, (4) triosephosphate. The samples of blood before the incubation (*G*), after 3 hr. (*F*), 6 hr. (*E*), 9 hr. (*D*), 12 hr. (*C*) and after 24 hr. (*B*) of incubation of blood at 37° C.

L. Macho

Endocrinological Institute of the Slovak Academy of Sciences, Bratislava.

[1] Cantarow, A., and Trumper, M., "Clinical Biochemistry" (Philadelphia, 1949).
[2] Macho, L., *Clin. Chim. Acta* (in the press).
[3] Paysant, P., and Wolf, R., *C.R. Soc. Biol.*, **146**, 1250 (1952).
[4] Mueller, C. B., and Hastings, A. B., *J. Biol. Chem.*, **189**, 881 (1951).
[5] Pappius, M. H., and Densted, O. F., *Canad. J. Biochem. Physiol.*, **32**, 293 (1954).
[6] Axelrod, B., and Bandurski, R. S., *J. Biol. Chem.*, **195**, 405 (1951).
[7] Hanes, C. S., and Isherwood, F. A., *Nature*, **164**, 1107 (1949).
[8] Macho, L., *Chemické Zvesti*, **11**, 175 (1957).
[9] Rohdewald, M., and Weber, M., *Hoppe-Seyler's Z. Physiol. Chemie*, **306**, 95 (1957).

Classical Motion under a Morse Potential

Students of diatomic molecules and of related systems have long used the Morse potential function[1]

$$V(x)=D\{1-\exp(-ax)\}^2 \qquad (1)$$

where x is the stretch of the interatomic bond (with $V=0$ at the equilibrium configuration $x=0$), D is the dissociation energy, and a a constant parameter. For energies less than D and no rotation, Morse gave the quantum energy levels of (1), namely

$$E_n=(n+\tfrac{1}{2})h\nu_0-\{(n+\tfrac{1}{2})h\nu_0\}^2/4D, \quad n=0,\ 1,\ 2,\ldots \qquad (2)$$

where $\nu_0\equiv(a/2\pi)(2D/\mu)^{\frac{1}{2}}$ is the frequency of classical small vibrations, μ being the reduced mass of the two bonded atoms.

Just as the quantum levels (2) are closely related to those of the harmonic oscillator, so also there is a close relation between the classical Newtonian motion under (1) and that of the harmonic oscillator. I found that Prof. Morse was aware of this; but he suggested that it should be made more widely known. The classical energy equation for the relative rectilinear motion of the two atoms is

$$\tfrac{1}{2}\mu(\mathrm{d}x/\mathrm{d}t)^2+D\{1-\exp(-ax)\}^2=E \qquad (3)$$

If the energy E is less than D, then integration (for example, using $\exp(ax)$ as variable) gives

$$ax=\log[\{1-\cos\theta\cos(2\pi\nu_0\, t\sin\theta)\}/\sin^2\theta] \qquad (4)$$

where $\cos^2\theta=E/D$, and the time t is measured from the position of minimum x. Thus the classical motion is periodic, and may be described as the logarithm of simple harmonic motion. The frequency of vibration at energy E is, from (4),

$$\nu=\nu_0\sin\theta=\nu_0\{(D-E)/D\}^{\frac{1}{2}}$$

tending to zero as E approaches D. If E has a value E_n as in (2), the classical motion has frequency

$$\nu=\nu_0\{1-(n+\tfrac{1}{2})h\nu_0/2D\}$$

depending linearly on the quantum number n.

For an energy E greater than D, the classical motion found from (3) is

$$ax = \log[\{\cosh\theta\cosh(2\pi\nu_0 t\sinh\theta) - 1\}/\sinh^2\theta)]$$

where now $\cosh^2\theta = E/D$. This non-oscillatory motion corresponds to dissociated states. The intermediate case $E = D$ gives classically

$$ax = \log\tfrac{1}{2}\{1 + (2\pi\nu_0 t)^2\}$$

This classical picture may usefully supplement the quantum-mechanical results.

N. B. Slater

Department of Mathematics,
The University, Leeds.
Sept. 2.

[1] Morse, P. M., *Phys. Rev.*, **34**, 57 (1929).

Prediction of Critical Temperatures

In cases where critical temperatures are unknown they can be calculated from a number of empirical or semi-empirical formulæ[1], the simplest but least-accurate being Guldberg's rule. More accurate equations exist for estimating values for hydrocarbons, for example, those of Jatkar and Lakshminarayanan[2] and Watson[3], but these are unsuitable for use with phenolic and basic organic compounds which occur in coal tar.

The critical temperatures of fourteen paraffins, twenty-five aromatic hydrocarbons, four phenols and seven organic bases[4–6] have been correlated in these laboratories with the boiling point and density of the respective compounds[7,8] by the method of least squares. As a result it was found that the following equation predicts values in the range 260–530° C. with an accuracy of ±20·8° C., that is, with an average of ±5 per cent, with 95 per cent confidence:

$$t_c = 221{\cdot}6 + 1{\cdot}029\ t_b\ d_{20}$$

where t_c is the critical temperature (°C.), t_b is the boiling point (°C.), and d_{20} is the density at 20° C. (gm./ml.). (In the case of solids, liquid values were extrapolated back to 20° C.)

The major discrepancies are given by five hydrocarbons the omission of which reduces the limits of error to ±14·2° C.

D. K. H. Briggs
W. D. Drake

Research Laboratories,
Coal Tar Research Association,
Oxford Road,
Gomersal, Leeds.

[1] Partington, J. R., "An Advanced Treatise on Physical Chemistry", 646 *et seq.* (Longmans, Green and Co., London, 1949).
[2] Jatkar, S. K. K., and Lakshminarayanan, D., *J. India Inst. Sci.*, **28**, A, 1 (1946).
[3] Watson, K. M., *Indust. Eng. Chem.*, **23**, 360 (1931).
[4] "Selected Values of Physical and Thermodynamic Properties of Hydrocarbons and Related Compounds", A.P.I. Research Project 44 (1953).
[5] Doss, M. P., "Physical Constants of the Principal Hydrocarbons" (The Texas Co., New York, 1943).
[6] Ambrose, D., and Grant, D. G., *Trans. Farad. Soc.*, **53**, 771 (1957).
[7] Coal Tar Research Association, "The Coal Tar Data Book" (Gomersal, C.T.R.A.).
[8] Egloff, G., "Physical Constants of Hydrocarbons" (Reinhold Pub. Corp., New York, 1946).

X-Ray Microscopy of Human Dental Pulp Vessels

Microradiographic studies of the human dental pulp vessels were prompted by the inadequate anatomical information on the pulpal vascular patterns, and by the statement that these vessels could not be visualized radiographically[1]. However, it has been shown that fine-contrast media of particle size 0·1–0·5μ (for example, 'Thorotrast', 'Micropaque') can be introduced by suction injection into the human dental pulp vessels and their vascular patterns demonstrated microradiographically[2].

Good results have been obtained by contact microradiography using a standard Philips 'Norelco' X-ray diffraction tube and an Ehrenberg–Hilger microfocus tube, with an effective focal spot of 1 mm. and 0·04 mm. respectively. The contact method, however, is limited partly by the size of the X-ray source and the grain-size of the recording emulsion, while the resolution cannot exceed that of the optical system used for enlarging the X-ray negative.

Recently better resolution and contrast, with consequently sharper image definition of all the vessels in the dental pulp, have been obtained by the projection method, using the X-ray projection microscope developed by Cosslett and Nixon[3]. The marked primary magnification (up to × 200 or higher) obtainable with this instrument, coupled with the high resolution afforded by its point source of X-ray emission (less than 1μ), makes it possible to image the smallest capillaries within the human tooth with great clarity.

This X-ray microscope has distinct advantages over the optical microscope in such dental studies by virtue of its penetration and depth of field. Its great focal depth results in all parts of the specimen being in focus, and permits the taking of stereomicrographs by shifting the specimen laterally between two exposures.

A section of human dental (bicuspid) pulp imaged in juxtaposition to a piece of 1,500 mesh silver grid,

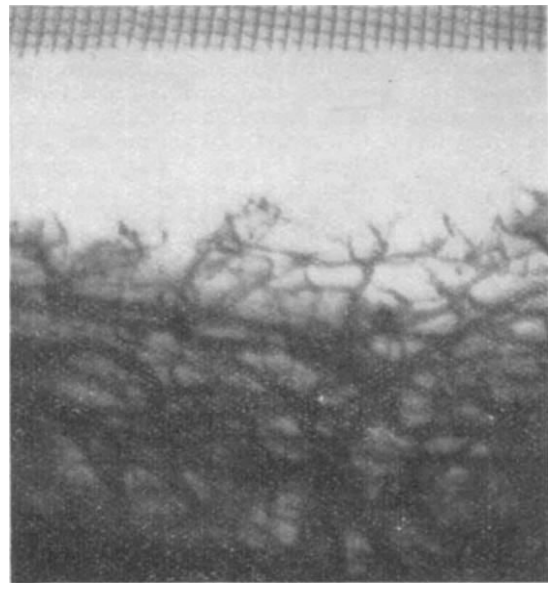

Fig. 1. X-ray micrograph of human dental pulp showing the capillaries of the subdentinal plexus imaged with 1,500 mesh silver grid